JOURNAL OF MAPS
2020, VOL. 16, NO. 2, 790–804
https://doi.org/10.1080/17445647.2020.1833768

Taylor & Francis
Taylor & Francis Group

Science



# Glacial geomorphology of the High Gredos Massif: Gredos and Pinar valleys (Iberian Central System, Spain)

Rosa M. Carrasco [a], Rodrigo L. Soteres [b,c], Javier Pedraza [d], Javier Fernández-Lozano [e], Valentí Turu [a,f], José Antonio López-Sáez [g], Theodoros Karampaglidis [h], José Luis Granja-Bruña [d] and Alfoso Muñoz-Martín [d,i]

[a]Department of Geological and Mining Engineering, University of Castilla-La Mancha, Toledo, Spain; [b]Instituto de Geografía, Pontificia Universidad Católica de Chile, Santiago, Chile; [c]Millennium Nucleus Paleoclimate, ANID Millennium Science Initiative, Santiago, Chile; [d]Department of Geodynamic, Stratigraphy and Paleontology, Complutense University, Madrid, Spain; [e]Prospecting and Mining Research Area, Department of Mining, Topography and Structure Technology, Higher Technical School of Mining Engineering, León, Spain; [f]Fundació Marcel Chevallier, Edifici Socio-Cultural de La Llacuna, Andorra la Vella, Principality of Andorra; [g]Environmental Archaeology Research Group, Institute of History, CSIC, Madrid, Spain; [h]MONREPOS, Archaeological Research Centre and Museum for Human Behavioural Evolution, Neuwied, Germany; [i]Instituto de Geociencias – IGEO (UCM, CSIC), Madrid, Spain

**ABSTRACT**

We present a detailed geomorphological map of the landform assemblages originated by the two major paleoglaciers of the Sierra de Gredos mountain range in the Spanish Iberian Central System. Based on previous works, our map focused on the features formed by Gredos and Pinar paleoglaciers during the last glaciation and subsequent glacial events. Based on a remote sensing analysis and exhaustive field surveys, we identified with great accuracy the local distribution of glacial, periglacial, mass movement, structural, fluvial, and lacustrine features. We recognized three main glacial geomorphological formations representing: (i) the maximum glacial extension reached (peripheral deposits); (ii) the culmination of glacial conditions (principal moraines) and (iii) the local glacial withdrawal (internal deposits). Our map offers a renewed spatial framework on which to conduct higher-resolution glacial chronologies, especially of Late Glacial and Holocene glacial activity, providing key information for performing future paleoclimatic reconstructions of the northern hemisphere mid-latitudes.

**ARTICLE HISTORY**
Received 27 May 2020
Revised 30 September 2020
Accepted 5 October 2020

**KEYWORDS**
Sierra de Gredos; glacial geomorphological mapping; last glacial maximum; last glacial termination; Holocene

## 1. Introduction

Mountain glacier activity is primarily controlled by temperature and precipitations (e.g. Oerlemans, 2005; Roe et al., 2017; Sutherland, 1984) and, therefore, the geomorphic records of former glacial pulses, such as moraine ridges and other ice-marginal landforms, reflect the occurrence of past climate conditions (Mackintosh et al., 2017). In this context, mapping in tandem with Terrestrial Cosmogenic Nuclide (TCN) exposure dating (Gosse & Phillips, 2001; Ivy-Ochs & Kober, 2008), have contributed to expand our knowledge of the sequence and synchronicity of past climate changes at a regional, hemispheric and global scale (Balco, 2011). The usefulness of geomorphological cartography in glacier chronology works using TCN and ice masses reconstruction has recently been highlighted, since for both it is essential to know the geomorphological context (Carrasco, Pedraza, Domínguez-Villar, Villa, et al., 2013; Ivy-Ochs & Kober, 2008; Pearce et al., 2017; Winkler, 2018).

The Sierra de Gredos is the most prominent mountain range in the Iberian Central System and their summits were occupied by extensive glaciers during the last glaciation (i.e. MIS 2; Palacios et al., 2011, 2012; Pedraza et al., 2013). Since this Mediterranean mountain runs in a W-E direction along the central sector of the Iberian Peninsula (Figure 1), is located under the influence of the northern westerly winds, which are considered a major component of the mid-latitude atmospheric circulation (Hurrell & Deser, 2009; Marshall et al., 2001). Deciphering the glacial activity in the Sierra de Gredos will provide insights into the atmosphere-ocean climate interactions occurred in the northern hemisphere mid-latitudes since the Late Pleistocene (Hughes & Woodward, 2008; López-Moreno et al., 2011).

The Main Map presented in this work is the result of research and experiences obtained in the context of several studies (Carrasco et al., 2015; Carrasco, Pedraza, Domínguez-Villar, Villa, et al., 2013; Carrasco, Pedraza, Domínguez-Villar, Willenbring, et al., 2013; Pedraza et al., 2013; Pedraza et al., 2019) aimed at establishing the morphostratigraphy, chronology, and reconstruction of the ice masses and evolution of the glaciers of the Upper Pleistocene of the Sierras

**CONTACT** Rosa M. Carrasco rosa.carrasco@uclm.es Department of Geological and Mining Engineering, University of Castilla-La Mancha, Avda. Carlos III, s/n, Toledo 45071, Spain

de Gredos and Guadarrama (Iberian Central System). On the other hand, both the methodology and the representation techniques used to prepare this cartography follow the most current trends for the elaboration of detailed geomorphological cartographies in glacial areas (see e.g. Campos et al., 2018; Leger et al., 2020; Lindholm & Heyman, 2016; Zasadni & Kłapyta, 2014).

## 2. Study area

### 2.1. Geographical and geological setting

The Sierra de Gredos is a intraplate mountain range located in the central sector of the Iberian Peninsula (~40° N; ~5° W), originating from the Alpine orogeny (mainly in the Neogene) by the reactivation of Late Variscan fractures resulting in a 'pop-up' structure and a stair-stepped topography (De Vicente et al., 2011; Pedraza, 1994). The High Gredos Massif is a tilted block mountain with uniform gentle northern slopes (2.3% general slope) and irregular steep southern slopes (18.5% general slope). The main ridge runs 6.8 km in NNE-SSW, NNW-SSE, NW-SE, and E-W directions forming the divide between the Douro and Tagus rivers basins. Some of the ancient pre-glacial erosion summit surfaces reach heights of around 2400 m a.s.l., culminating at 2592 m a.s.l. (Almanzor peak; 40° 14′ 45.52″ N; 5° 17′ 51.04″ W) (Figure 1).

The rivers Garganta de Gredos (Gredos Gorge; hereinafter Gredos river) and Garganta del Pinar (Pinar Gorge; hereinafter Pinar river) flowing from the summits of the High Gredos Massif (above 2400 m a.s.l.) to Tormes river (1217 m a.s.l.) and, during the Last Glacial Cycle, their valleys were occupied by two of the main glaciers of the Iberian Central System. The primary origin of these valleys is associated with two morphotectonic corridors (Gredos-Chilla and Pinar-Tejea gorges) due to fractures NNE-SSE and, to a lesser extent, N-S and NNW-SSE. Their evolutionary history throughout the Quaternary period is completed by pre-glacial fluvial denudation, glacial, and periglacial remodeling and post-glacial and current river action (Martínez de Pisón & Muñoz-Jiménez, 1972; Muñoz et al., 1995; Pedraza, 1994; Pedraza & Fernández, 1981). Hydrologically, both rivers are classified as 'torrent-type high mountain rivers with a nivo-pluvial regime' (CHD, 2012). The Pinar river is a tributary of the Gredos river and this, in turn, of the Tormes that is the main river in the northern slope of the High Gredos Massif and tributary of Douro, one of the main rivers of the Iberian Peninsula. The total surface area of the Gredos river drainage basin is 57.9 km$^2$, the maximum channel length is 16.12 km and the maximum and minimum elevations of the basin are 2591 (Almanzor peak: 40° 14′ 45.52″ N; 5° 17′ 51.04″ W) and 1217 m a.s.l (the mouth of the Gredos river into the Tormes river: 40° 20′ 48.93″ N; 5° 17′ 47.80″ W), respectively. In the headwater sector, corresponding to the former glacial cirques, the rivers flow on basement rocks (rocky bed rivers type) and with numerous rapids, while in the middle and lower sectors the rivers flow on gravel and other surficial deposits of the former glacial and pro-glacial valleys (gravel bed rivers type). Finally, it highlights the fact that the postglacial

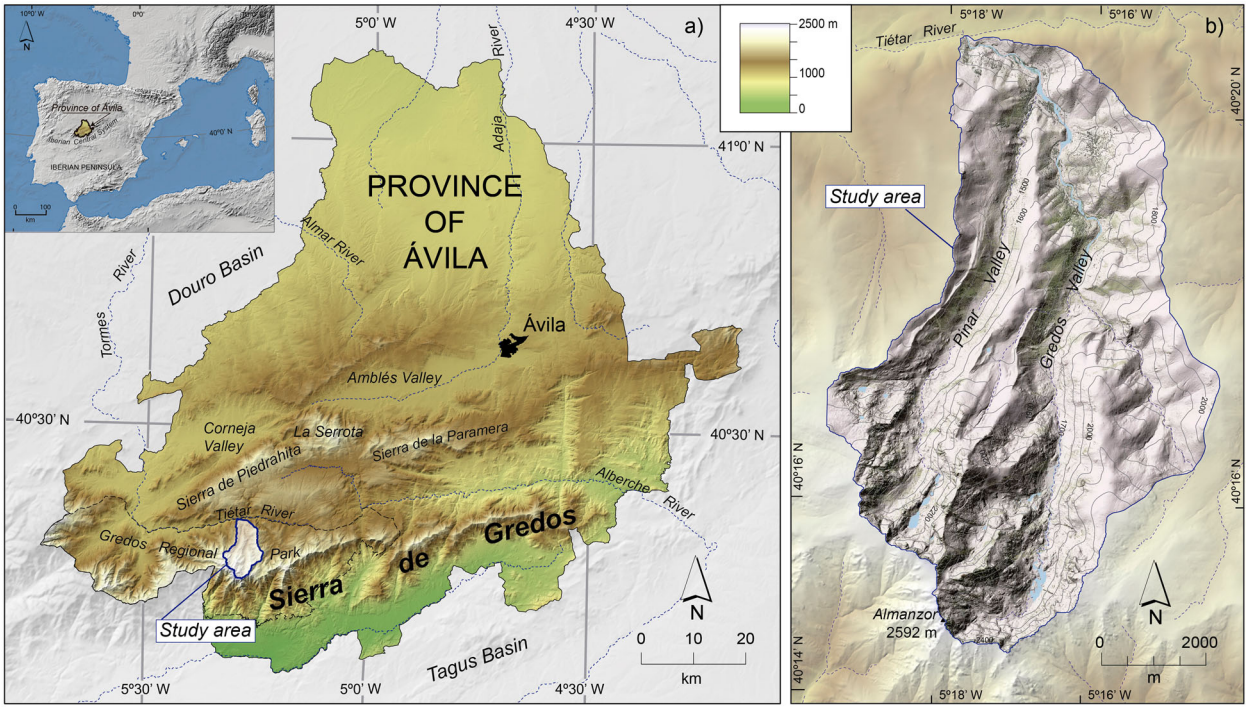


**Figure 1.** (a) Location of the Gredos Regional Park in the Province of Ávila. (b) Location map of the Gredos and Pinar valleys.

channels are narrow and slightly cut into the bedrock floor or into their previous deposits, so that they have hardly modified the morphology of the former glacier bed.

The predominant lithology of the area is composed by Variscan granitoids (i.e. monzogranites, granodiorites), pre-Variscan metamorphic rocks (gneisses, schists, slates, quartzites), and large surficial Quaternary deposits (i.e. alluvial, glacial, periglacial) (GEODE, 2004).

The area has a Mediterranean mountain type climate, strongly influenced by continentality (Köppen-Geiger Climate Classification Dsb and DsC; AEMET & IPMA, 2011; Durán et al., 2013). The surface climate of the Mediterranean region is primarily linked to the North Atlantic Oscillation (NAO) and also, to a lesser extent, to the Mediterranean Oscillation, the Western Mediterranean Oscillation and the East Atlantic Oscillation (Hurrell, 1995; Sánchez-López et al., 2016; Vicente-Serrano et al., 2009). Annual latitudinal migration of the Azores anticyclone allows the arrival of Atlantic depressions leading to cold and wet conditions during the winter season, while warm and dry summers occur in the region (Sánchez-López et al., 2015). In the area corresponding to the Gredos-Pinar river basin, the following climatic data range can be established from the summits (heights above 1400 m a.s.l.) to the piedmonts (heights around 1200 m) (AEMET & IPMA, 2011; Ninyerola et al., 2005): (i) the range of air temperature for the annual average varies from 2.5 to 12.5° C; for the maximum annual average varies from 10 to 17.5°C and for the minimum annual average from −2.5 to 2.5°C; (ii) the mean number of days $yr^{-1}$ with temperatures below 0°C ranges from100–120 to 80–100; and (iii) the range of average total annual precipitation reaches1800–700 mm. Above 2000 m a.s.l., the snow cover persists between 180 and 300 days $yr^{-1}$ on discreet sectors sheltered by the local topography (Muñoz et al., 1995).

### 2.2. Previous work

Although almost all the works on the glacial morphology of High Gredos Massif contain some kind of graph, scheme or map, the most complete cartographies of this area are those corresponding to the Quaternary deposits elaborated in the context of the Spanish Geological Map (Pedraza & Fernández, 1981), those of glacial morphology of the Gredos and Pinar gorges associated with chronological studies (Palacios et al., 2011, 2012) and that of the Gredos Cirque associated with a study on snow avalanches (Soteres, Pedraza, et al., 2020). Although all the data contained in these maps have been fundamental to carry out this work, it is the avalanche map that most coincides with the objectives presented in this work due to its methodology and technique of preparing the different maps.

Early references to the glacial landscape of the Sierra de Gredos go back to the late nineteenth century (Baysselance, 1884; de Prado, 1862; Penck, 1894). However, first systematic studies focusing on the glacial landforms of the region were carried out in the early twentieth century. Schmieder (1915), Huget del Villar (1915), Obermaier and Carandell (1916) and Vidal Box (1932, 1936) described, and occasionally mapped, the major morphological features of these areas. Furthermore, according to geomorphic-based paleoglacier reconstructions, Obermaier and Carandell (1915) also suggested a snowline altitude for the Quaternary period, conducting one of the first paleoclimatic inferences for the Iberian Central System. Decades later, geomorphological mapping of the High Gredos Massif was significantly improved by Martínez de Pisón and Muñoz-Jiménez (1972). Afterwards, Pedraza and Fernández (1981) performed the detailed mapping of the glacial deposits in these areas. The first detailed geomorphological mapping of the High Gredos Massif was presented by Muñoz et al. (1995), Palacios and Marcos (1996) and Palacios et al. (2011, 2012). Outside the High Gredos Massif, Carrasco, Pedraza, Domínguez-Villar, Villa, et al. (2013) reconstructed the extent of the plateau ice-cap that occupied the nearby Sierra de Bejar and Pedraza et al. (2013) established a conceptual model of the evolutionary stages of the glaciers in the Sierra de Gredos during the last glaciation. More recently, using the most up-to-date procedures Campos et al. (2018) mapped in detail the glacial morphology of the main gorges across the nearby Sierra del Barco or La Nava.

First comprehensive chronologies of glacial fluctuations in the Sierra de Gredos using $^{36}$Cl-TCN exposure dating were carried out by Palacios et al. (2011, 2012). The results indicated that the Gredos paleoglacier reached its outermost glacial limit at ~26 ka, coeval with the global LGM, the onset of local deglaciation at ~21 ka and at ~16 ka the glacier front withdrew near to its headwall (Palacios et al., 2011). The age of past fluctuations of Pinar paleoglacier was ~24 ka for the outermost glacial limit, also contemporaneous with the global LGM, at ~17 ka beginning of the local deglaciation and at ~10 ka place the complete disappearance of the glacier (Palacios et al., 2012). These data agree with those obtained using $^{10}$ Be-TCN exposure dating in the Cuerpo de Hombre paleoglacier (Sierra de Béjar, western sector of Sierra de Gredos, 40 km west of High Gredos Massif). In this paleoglacier, a complete sequence was obtained from the LGM to the Holocene with well-marked Late Glacial stages and correlated with different mountains at the peninsular and continental level (Carrasco et al., 2015). This record, validated with $^{14}$C dating and pollen studies (López-Sáez et al., 2020; Turu et al., 2018), constitutes the first direct evidence

of complex glacial activity during the Late Glacial in the Iberian Central System. Recently, a set of cosmogenic ages obtained in previously glaciated valleys of the Sierra de Gredos have been summarized in Oliva et al. (2019), who also recalculated all the available chronological data of the Iberian Peninsula considering the most accurate and up-to-date TCN production rates.

## 3. Methodology

In order to perform rigorous mapping of the spatial distribution of the glacial landforms created by both the Gredos and Pinar paleoglaciers, we conducted a combination of pre-field photointerpretation map (made using panchromatic stereo-photos) and field checking (Chandler et al., 2018; Evans, 2012; Seijmonsbergen, 2013; Smith et al., 2006; Verstappen, 2011). Using as a basis the classical structure of the legend for geomorphological maps (landform/deposit-process-age represented by symbols and colors patterns; Demek, 1972) and the most standardized symbols (FGDC, 2006), we first produced a preliminary map by using ArcGIS 10.4 software and 3D imagery of the IBERPIX visor (IGN-IBERPIX). In order to identify minor glacial features, we also examined aerial imagery (spatial resolution 0.5 m) and the LIDAR (Laser Imaging Detection and Ranging) digital terrain model (DTM, spatial resolution 0.2 m) both provided by the PNOA (Spanish National Program for Aerial Orthophoto). All geographic data was compiled from the Spanish National Center for Geographic Information (IGN-CNIG, www.ign.es). LIDAR derived DTMs were processed following the methodology proposed by Fernández-Lozano et al. (2015) based on the algorithms implemented by Kokalj et al. (2011), which have yielded promising results in the analysis of surface processes and minor landforms in archaeological works (Fernández-Lozano et al., 2020). However, we adapted this twofold approach for mapping glacial landforms. The workflow consisted in the generation of a slope and Simple Local Relief Model (SLRM) maps. While slope maps represent the maximum rate of change between DTM neighbors cells by determining the difference of solar illumination provided by ridges and talwegs, the SLRM map enhances the visibility of low relief features by removing large-scale landforms from the original DTM (Hesse, 2010). Both types of maps proved to be a useful guideline for mapping glacial geomorphological features such as moraines and cirques, especially the headwall, by providing variations in shading and hue between different small and large relief elements (Figure 2). Finally, we conducted exhaustive field surveys to check out our preliminary map by using a handheld GPS.

## 4. Results

We grouped together local geomorphological features according to their morphogenetic nature in glacial, periglacial, mass movement, fluvial and lacustrine landform assemblages. Individual landforms are summarized in Table 1, adapting the scheme presented in Darvill et al. (2014), Bendle et al. (2017) and Soteres, Peltier, et al. (2020).

### 4.1. Glacial landforms

The landscape of the High Gredos Massif is dominated by both erosional (i.e. cirques, U-shaped valleys, roches moutonnées) and depositional (i.e. moraine ridges) glacial features, which are clearly preserved between ~2400 and 1400 m a.s.l.

The former accumulation zones of these glaciers were located close to the main summits. They present the characteristic appearance of glacial cirques, that is to say, semi-circular hollows bounded by steep slopes (Evans & Cox, 1974), but, in general, their morphology is more complex than that of the cirques described in easternmost areas of the Iberian Central System (Pedraza et al., 2019). The two larger ones, Gredos (total surface 1356 ha; bottom elevation from 1650 to 2000 m a.s.l.; average length of headwalls 350 m) and Pinar (total surface 680 ha; floor elevation from 1700 to 1960 m a.s.l.; average length of headwalls 300 m), are complex cirques formed by four and three compartments, respectively. The third, La Hoya del Cervunal, is a smaller (total surface 33 ha; bottom elevation from 1900 to 2000 m a.s.l.; average length of headwalls 100 m) and simple cirque. Major cirques often show glacial thresholds as well as well-defined arêtes and horns (Figure 3).

The Gredos gorge runs in a N-S and NW-SE directions and reaches ~8.5 km in length, ~1.0 km width and ~350 m in depth. The Pinar gorge runs in a N-S and NNE-SSW directions and has ~10 km in length, it is ~1.2 km in its widest stretch and ~400 m in depth. They both present a typical U-shaped profile, although some portions have been subdued by post glacial slope deposits (Figure 4). Close to their headwalls, the floor of both gorges is predominantly rocky, exhibiting a well-preserved ice-sculpted topography. Several polished bedrock outcrops show the typical asymmetric profile of the *roches moutonnées* with the steepest slope facing north. Frequent glacial striations and both isolated or aligned erratic boulders occur over the ice-sculpted bedrock features (Figure 5(a), 5(b)).

Ice-marginal features, especially moraines, are well represented on the slopes in both Gredos and Pinar valleys between ~1800 and ~1400 m a.s.l. (Figures 4 and 5 (c)). These landforms are positive-relief linear features composed of fine to coarse sediments,

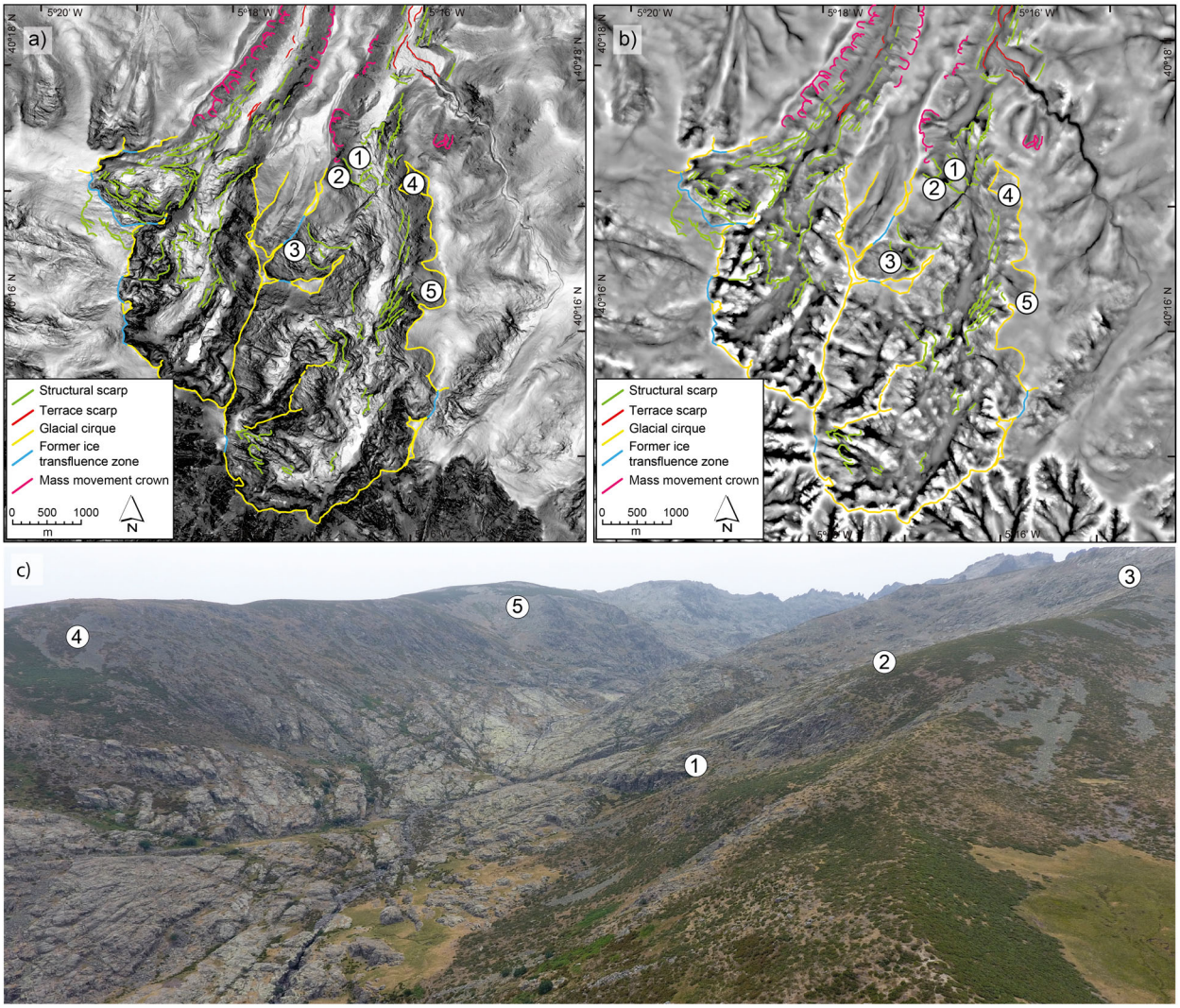


**Figure 2.** (a) Slope map of the study area. (b) SLRM map with radial curvature of 20°. (c) Aerial image of the Gredos valley view from the N, showing the view-eyed position indicated in (a) and (b).

including several metric-scale boulders, which delimitate the extent of former glaciers. Major moraines in the study area can reach ~4 km in length and ~250 m in height from the valley bottom. Associated with the distal slope of the main moraine we identified aligned boulder trains partially buried by glaciofluvial deposits. Further into the main moraine, we identified a sequence of at least 11 and 14 minor moraine ridges in the Gredos and Pinar gorges, respectively. In the interfluve between the main valleys, the smaller Hoya Nevada paleoglacier originated a sequence of at least 9 minor moraine ridges distributed between ~1900 and ~1800 m a.s.l.

Upstream, ice-marginal features are scarce and only occur as diffused groups of aligned boulders and minor moraine ridges with a transverse orientation related to the inferred ice flow direction. These glacial limits appear at the bottom of the Gredos and Cinco Lagunas cirques at elevations of ~2000 m a.s.l.

According to their morpho-stratigraphic and evolutionary significance (Pedraza et al., 2013) and their chronology (Palacios et al., 2011, 2012; recalculated in Oliva et al., 2019), all these moraine systems and their corresponding ridges have been grouped together into three main formations (Figures 4 and 5 (c)): (1) peripheral deposits (PD; ~26–24 ka), (2) principal moraines (PM; ~24–20 ka) and (3) internal deposits (ID; ~20–12 ka). The PD formation consist of scattered erratic boulders and minor moraines and correspond to the outermost ice-marginal features. It represents the most extensive glacial stage, including the Glacial Maximum and subsequent limited retreat. The PM formation is the most outstanding lateral moraines rimming the valley and they were developed during a stage of remarkable readvance and subsequent stabilization of local paleoglaciers, representing a valuable morpho-stratigraphic marker for the LGM. Finally, the ID formation is composed by scattered erratic boulders and minor recessional moraines (latero-frontal or arcuate) located near the headwalls. This formation marks different events of glacier retreat during the deglaciation phase and includes short stages of glacier stabilization, probably correlated with the three Dryas stadials.

**Table 1.** Summary of the glacial and associated landforms of Gredos and El Pinar valleys (1).

| Morphogenetic System | Process or paleo-process / Landform[1] | | Morphology and interpretation | Chronology or stage |
|---|---|---|---|---|
| 1. Glacial | Aggradation | *Peripheral Deposits* Figures 4(a), 5(c) | Scattered erratic boulders and minor moraines with a maximum height of 6 m above the level of the Cervunal meadows. They correspond to the Glacial Maximum advance and subsequent limited retreat stages. | ~26–24 ka [2] |
| | | *Principal Moraine* Figures 4(a),4 (b), 5(c) | The most outstanding lateral or border moraines that limit the valley with a maximum height of 50 m above the level of the Cervunal meadows and 250 m above the level of the valley bottom. They correspond a stage of remarkable re-advance and stabilization of glaciers. | ~24–20 ka [2] |
| | | *Internal Deposits* Figures 4(b), 4(c), 5(c). *General* | System scattered erratic boulders and recessional minor arcuate or latero-frontal moraines 1.5–10 m high, respectively, a maximum height above the level of the valley bottom. They represent the stages of glacier retreat associated with the deglaciation phase. | ~20–12 ka [2] |
| | | *Supra-glacial till deposits* | Massive concentration of boulders in the valley bed showing moraine arcuate crests. Their structures, such as, fractured 'megaclasts', pervasive jigsaw textures and sedimentary contrast between their proximal and distal reaches, are indicators of a primary origin by rock avalanches onto glaciers. | |
| | | *Basal complex formation* Figures 4(b), 4(c), 5(d) | Plains with hydromorphic soils and grassland development, which represent the result of a complex sedimentary filling in which sequences of tills, fluvioglacial and lacustrine deposits may appear. | |
| | | *Moraine ridge* Figures 4(a), 4(b), 5(c) | Summit of elongated hill or boulder alienation | From the Glacial Period to the Present Time |
| | Erosive | *Polish and striated bedrocks* Figures 5(a), 5(b), 6(d) | Abrasive structures on the granite rock surface of a former glacier bed. These structures have a remarkable development on the thresholds of the Laguna Grande cirque. | During the glacial stages |
| | | *Glacial cirque* Figures 3, 5(a), 6(c) y 6(d) | The two larger one, Gredos (1356 ha) and El Pinar (680 ha), are complex cirques formed by four and three compartments, respectively. The third, La Hoya del Cervunal, is a smaller (33 ha) and simple cirque. | |
| | | *Former ice transfluence zone* Figure 3 | A relatively low topography on the summit surface or ridge line (saddle topography) connecting two former ice accumulation basins or glacial cirques. | During the stages o expansion of ice (~26–20 ka) |
| 2. Periglacial | Aggradation | *Protalus (or pronival) rampart* Figure 6(a) | These are boulder ridges produced at the lower margins of perennial or semi-permanent snow beds located on the upper threshold beneath of headwalls of the cirque (from ~2350 to 2400 m asl) | The probable maximum of activity during the Little Ice Age [3] |
| | | *Protalus ridge* | | |
| 3. Mass Movement | Aggradation (deposits) | *Talus Slope* Figures 5(a), 6(a), 6(c) | These are widespread in the upper sector of the gorges, commonly associated with the base of major rock cliffs or cirque headwalls. In many cases, talus slopes are formed by coalescence debris fans | In general, they are paraglacial slope phenomena whosemaximum activity takes place during deglaciation (~20–12 ka) and first postglacial (Lower Holocene) stages, with a remarkable attenuation at present. |
| | | *Debris avalanche* Figure 4(a) | Located on the lateral moraines. Usually these formations are small, however we recognized a major avalanche in the left lateral moraine of the Gredos gorge, close to the Cervunal area (Navazarza site). | |
| | | *Debris Flow* Figure 4(a), 6(b) | Debris flows can occur at both rocky and loose sediment slopes, coinciding with the cirques and the moraines and talus, respectively. The largest debris flows typically occur associated with structural corridors located at the headwalls, reaching ~400 m in length. The major concentration of these landforms appears in the proximal slope of the El Pinar Moraine. | |
| | | *Solifluction-gelifluction* Figure 7(b) | These phenomena are frequent in areas of weathered rocks (grus) and concentrations of fine-grained materials (subglacial till and hydromophic soils) and they consist of lobes, sheets and tongues of small dimensions (2–5 m). | Pleistocene pre-Last Glacial Cycle at present |

(*Continued*)

**Table 1.** Continued.

| Morphogenetic System | Process or paleo-process / Landform[1] | | Morphology and interpretation | Chronology or stage |
|---|---|---|---|---|
| | Erosive | *Crown and main scarp* Figure 4 (a) | Semi-circular scarps on the headwalls of a mass-wasting deposits reaching the floor of the valley. The most significant of these morphologies corresponds to the Navazarza avalanche. | |
| 4.Structural and mixed | Erosive | *Fracture zones and corridors* Figure 6(a), 6(d) | Pre-glacial morphologies derived from tectonic reactivation and modified by fluvial, periglacial and glacial processes. The ones represented here correspond mainly to glacial and periglacial activity | Upper Pleistocene and Holocene. |
| | | *Fault-line scarp and threshold* Figure 6(a), 6(d) | | |
| 5. Glacio-Fluvial | Aggradation | *Proglacial alluvial plain* Figure 4(b) | Paraglacial phenomena resulting from melting and ablation of the glaciers. Located at the bottom of the valley, these formations can be correlated with those of internal glacial deposits (ID). | During the deglaciation (~20–12 ka) [4] |
| | | *Proglacial alluvial fan* Figures 4(a), 4(b) | | |
| 6. Fluvial | Aggradation | *Alluvial terrace* Figure 4(b) | These landforms are discontinuous and appear on both sides of the channel and only in the two main rivers, Gredos and El Pinar. In general, they are embedded in the bottom of the former glacial valley on the basal complex formation (BC) and the former fluvioglacial floodplain | Post-glacial (Holocene) |
| | | *Alluvial fan* Figures 4(a), 4(b) | These landforms are associated with debris flow channels as evolutionary stages subsequent to them or to former proglacial alluvial fans as new sequences of progradation. They mainly appear on both sides of the valley in the foot slopes of moraines. | |
| | Mixed | *Fluvial plain (river channel and floodplain)* Figure 4 | The two only rivers that have a large alluvial plain are Gredos and El Pinar. These landforms are the generalized current channels and their floodplain with discontinuous development and made of gravel bar braid. The alluvial plain is embedded in the bottom of the former glacial valley on bedrock polished surfaces or previous surficial deposits. | |
| | Incision | *Terrace and channel Wall* Figure 4(b) | Recent and ancient riverbank scarps | |
| 7. Lacustrine | | *Lakes and ponds* Figures 3, 4(a), 7 | Most were caused by glacial overdeepening in the former accumulation basin (cirque lake) and only one (La Laguna del Cervunal) is a moraine-dammed type. They vary between true perennial lakes (in general, greater than 0.5 ha in surface area and 3 m in depth) and small seasonal lakes or ponds. | From the early stages of retreat (moraine dammed lakes, after ~26 ka) or the Finiglacial stages (cirque lakes, ~12 ka) to the present. |
| | Aggradation | *Peaty system* Figures 4(a), 5(d), 7(b) | These landforms are created by the sediment overfilling in former lacustrine basins or similar depressions. They are a flat surface colonized by herbaceous vegetation forming small grasslands (locally known as *cervunales* and *navas*). | From pre-Last Glacial Cycle (Pleistocene) to Present Time |

[1]The colors and symbols used here are those used in the general geomorphological map.
[2]Absolute chronology provided by $^{36}$CL-TCN (Palacios et al., 2011, 2012; recalculated in Oliva et al., 2019).
[3]Provided by lichenometric analysis (Sancho et al., 2001).
[4]Absolute chronology provided by Optically Stimulated Luminescence for some deposit (Muñoz-Salinas et al., 2013).

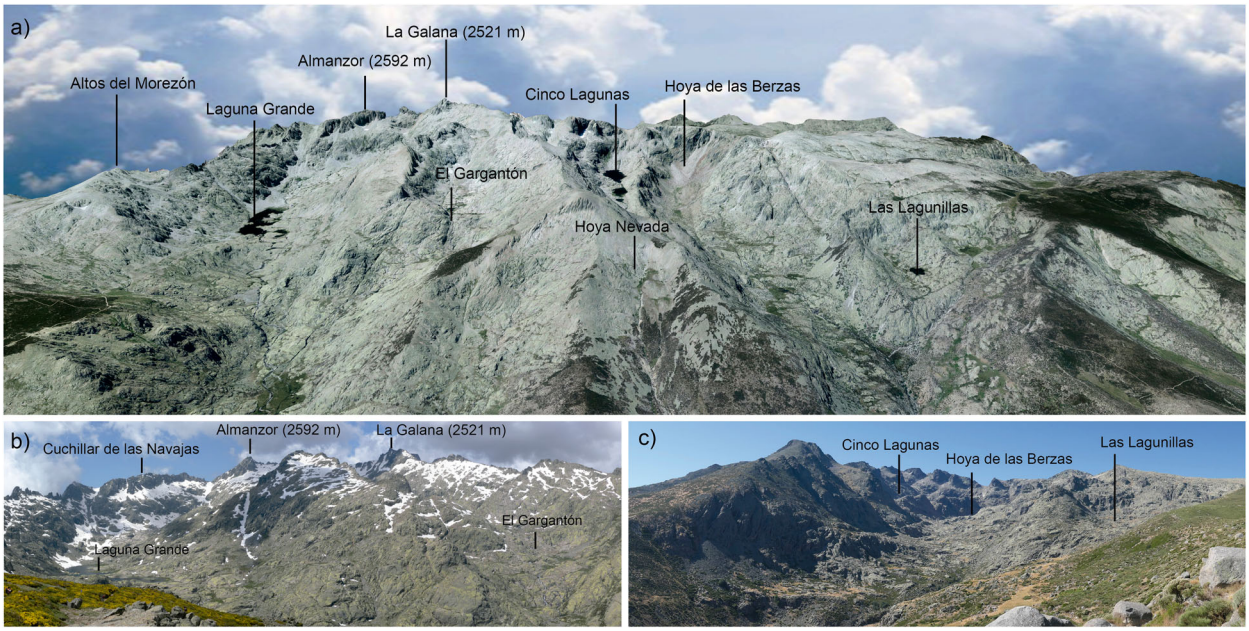


**Figure 3.** (a) Aero-3D reconstruction based on the combination of 5 m LiDAR data and aerial ortophotograph (www.ign.es) of the Gredos and Pinar cirques. Horizontal photographic view from the N of Gredos (b) and Pinar (c) cirques. As the three images show, these are complex cirques formed by several compartments: La Laguna Grande and El Garganton in the Gredos cirque; and Cinco Lagunas, Hoya de las Berzas and Las Lagunillas in the Pinar cirque.

Finally, the term 'basal complex' (BC) is introduced here to account for the sedimentary sequences forming flat morphologies located along the valley floor, which has generally been classified as 'ground moraine'. These formations result in a sequence of sedimentary filling processes in some small basins or subglacial concavities (80–500 m long and 1–4 m deep). The most complete sedimentary sequence comprises (from bottom to top): subglacial till (lodgment and melt-out) and supraglacial till (generally, ablation till), fluvioglacial sediments, peaty sediment and hydromorphic soils (BC, Figures 4 (b), 4(c) and 5(d)).

### 4.2. Nival and periglacial landforms

The periglacial dynamic in the Sierra de Gredos had remarkable activity and efficacy during the cold stages of the Upper Pleistocene and Holocene (Acaso et al.,

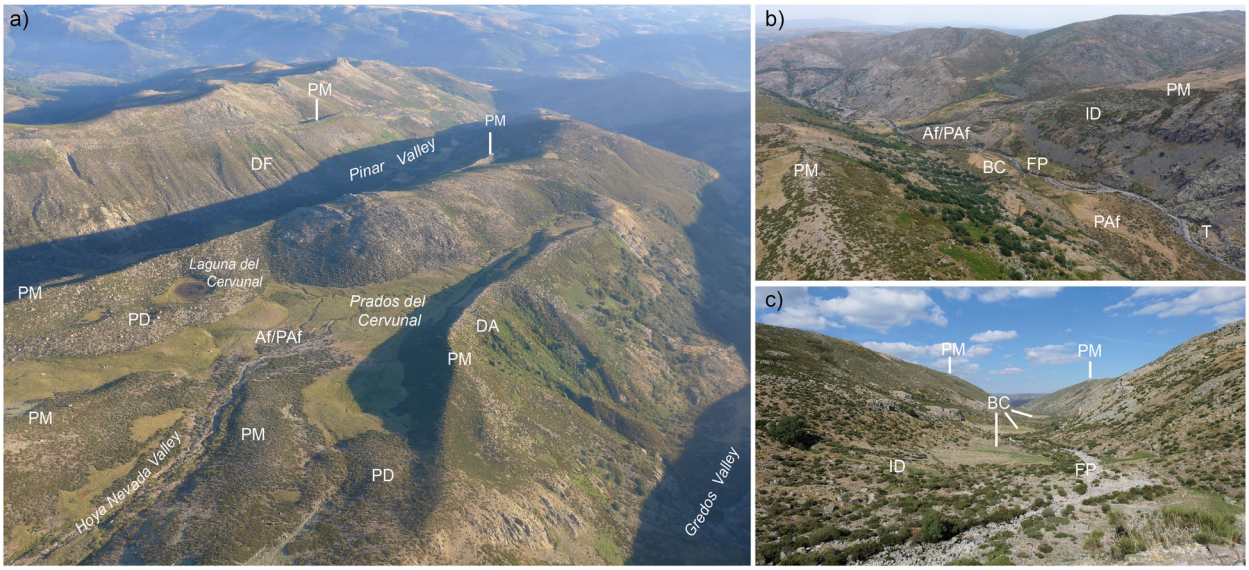


**Figure 4.** (a) General view from the S of the Gredos and Pinar gorge valleys with their lateral moraine complexes (peripheral, principal and internal formations; PD, PM and ID, respectively), the intramorainic meadows and peaty system (*nava*) of Prados del Cervunal and a series of ancient and recent (from ~11 ka to present; Muñoz-Salinas et al., 2013; Palacios et al., 2012) debris-flow (DF) and debris avalanche (DA) on the slopes of lateral moraines. (a) and (b) (Af/PAf) postglacial and proglacial alluvial fans superimposed. (b) and (c) The Gredos and Pinar valleys, respectively, showing their U-shaped morphology, the lateral moraine complexes (principal and internal formations, PM and ID, respectively), basal complex (BC), proglacial alluvial fans (PAf), alluvial terrace (T) and postglacial fluvial plain features (FP).

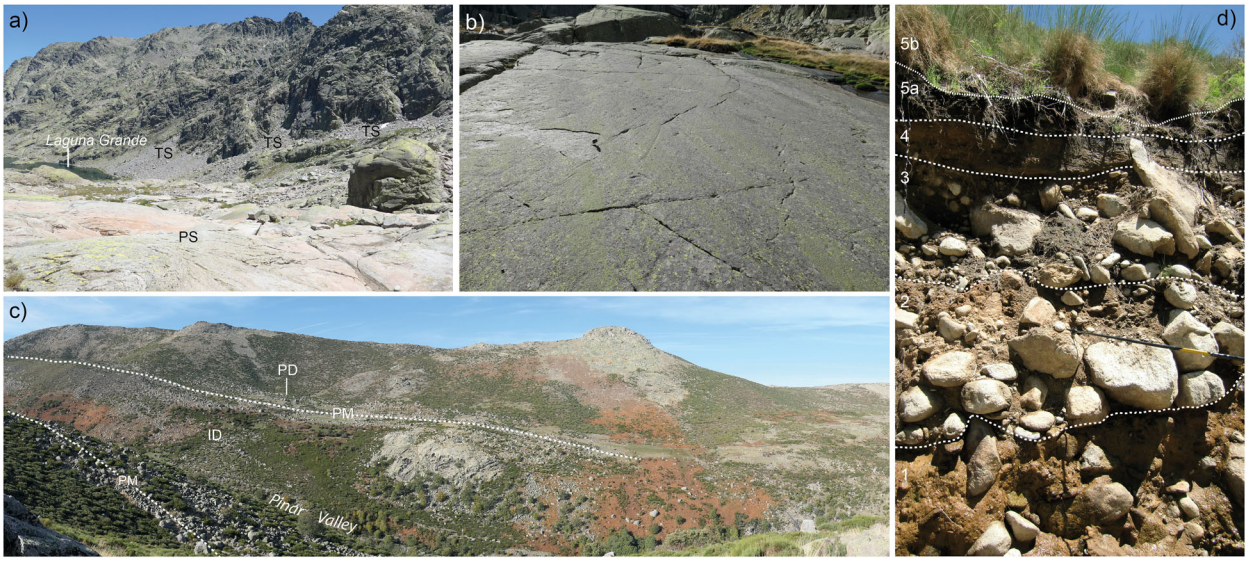


**Figure 5.** Glacial deposits and landforms. (a) General view from the SW of the floor of Gredos cirque showing the granite bedrock eroded by glacial abrasion (PS, polished surface; TS, talus slopes); (b) A detailed view of striations and polished surface in the Gredos cirque bedrock. (c) General view from the NE of morainic formations of Pinar paleoglacier: PD, peripheral deposit formation; PM, principal moraine formation; and ID, internal deposit formation. (d) The sedimentary basal complex (from the bottom to top): 1, Subglacial lodgement till; 2, Subglacial melt-out till; 3, Supraglacial ablation till; 4, Proglacial lacustrine sediments; 5a, Postglacial hydromorphic soils; 5b, grassland of *Nardus stricta* and *Festuca indigesta* (*navas* or *cervunales*).

1986; Martínez de Pisón & Palacios, 1997; Muñoz et al., 1995; Pedraza, 1994). After the LIA, the periglacial activity had a noticeably declined being driven by seasonal and diurnal frost formation of incipient solifluction landforms above 1850 m and micro patterned ground above 1600–2000 m (Oliva et al., 2016). Of all these types of periglacial landforms, in the Gredos and Pinar gorges area only the formations of debris accumulations have been identified with cartographic entity. For the reasons set out in the corresponding section, part of these formations has been included as mass movements, leaving here those genetically associated with snow processes.

The main geomorphic features related to nival processes in the study area are protalus or pronival ramparts (PR; Figure 6(a)). These landforms are defined by a ridge or ramp formed by coarse debris at the downslope margin of a perennial or semi-perennial snow patch (Shakesby, 1997). Their formation is commonly attributed to debris originated by freeze–thaw processes in nearby bedrock cliffs, which fall and roll over the snow patch to accumulate in its limit (Ballantyne & Benn, 1994; Matthews et al., 2017).

In the Gredos gorge, these periglacial landforms were first identified by Muñoz et al. (1995), who recognized the most impressive protalus rampart in the main cirque walls, specifically in the Cuchillar de las Navajas area. Subsequently, Sancho et al. (2001) carried out a lichenometric analysis at the site and concluded that this feature was most likely formed during the Little Ice Age. Additionally, the authors also identified protalus ramparts in the northeast face of the Almanzor peak, the Canal de la Portilla, El Gargantón gorge and El Cervunal cirque. In Pinar gorge, Palacios et al. (2012) recognized two protalus ramparts nearby La Galana and Güetre peaks.

### 4.3. Mass movement landforms

Erosive and depositional landforms associated with slope failure processes are common in the study area. We prefer to classify them as mass movement landforms because there are several processes involved on the denudation of the rock walls which provide sediments for the formation of these features (i.e. freeze–thaw, hydrostatic pressure, structural and lithological arrangements and, probable, debuttressing).

Debris flow features (DF; Figures 4(a) and 6(b)) are widespread in both gorges (Muñoz et al., 1995; Muñoz-Salinas et al., 2013; Palacios et al., 2012; Palacios & Marcos, 1996). These landforms consist of a small failure escarpment in their upper sector, associated with a narrow and deeply incised channel and, occasionally, a fan deposit in their lower section. Debris flows can occur on both rocky and loose sediment slopes, coinciding with cirques and moraines or talus slopes, respectively. Largest debris flows typically occur associated with structural corridors, reaching ~400 m in length. The major concentration of these landforms appears in the proximal slope of the Pinar principal moraine.

Talus slopes (TS; Figure 6 (c)) are formed by the accumulation of angular heterometric debris resting at a ~35° angle located at the base of major rock cliffs. In many cases, talus slopes are composed by

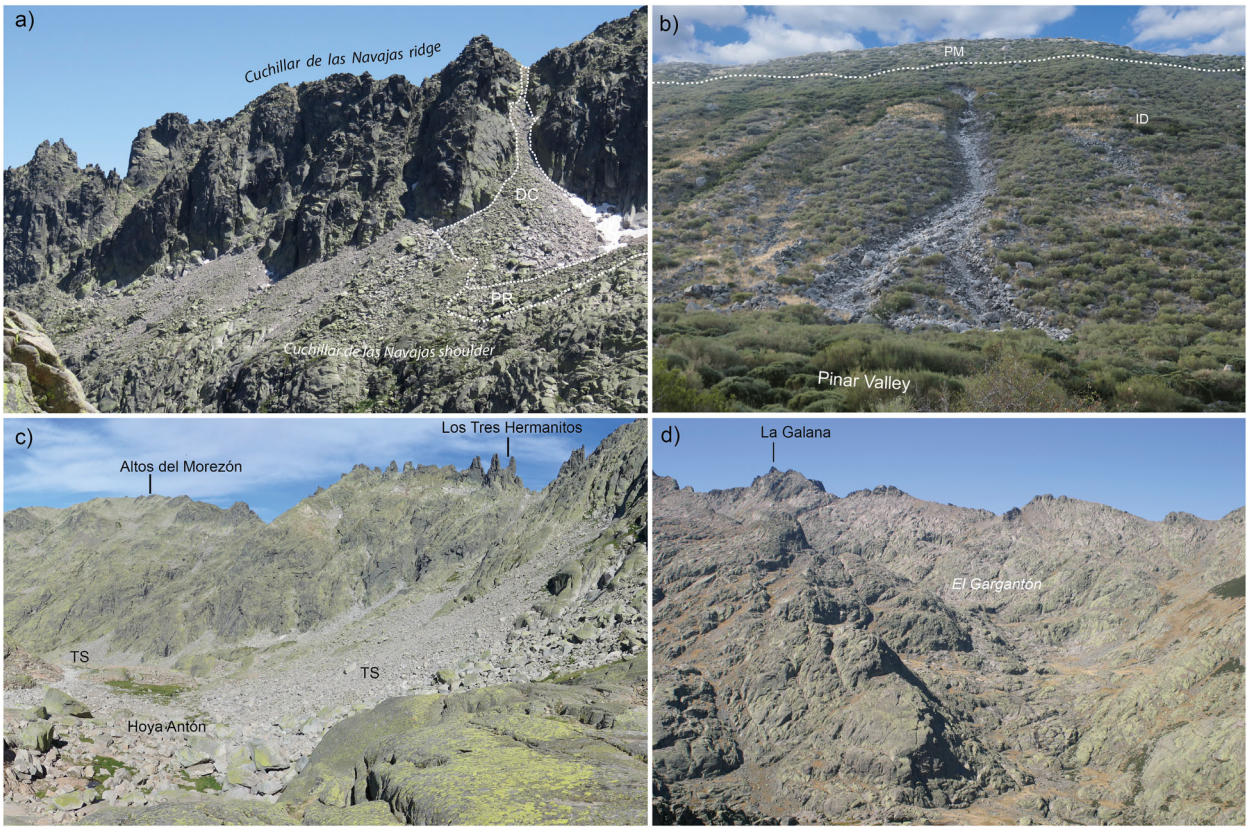


**Figure 6.** (a) Protalus rampart (PR) partially fossilized by a subsequent debris cone (DC), located on one shoulder of the Gredos cirque slopes and associated with fracture corridors, view from the NW. (b) Recent debris flow on the slopes of lateral moraines of Pinar paleoglacier. (c) Talus slopes (TS) located at the foot of the Gredos cirque walls. (d) Polished surfaces, thresholds, fault lineaments, corridors and escarpments on granite bedrock of the El Garganton, view from the NE (Gredos cirque, see Figure 3).

coalescence debris fans, which are formed by punctual rockfalls channeled along the structural corridors (Figures 5(a), 6(a) and 6(c)). These landforms are ubiquitous in the upper sector of both valleys.

Additionally, in the Pinar gorge, we identified a massive supra-glacial till deposit similar to that described in the paleoglacier of the Cuerpo de Hombre formed by a former rock avalanche event (paraglacial debuttressing processes; Carrasco, Pedraza, Domínguez-Villar, Willenbring, et al., 2013). This feature is characterized by a thick accumulation of angular heterometric debris distributed on arcuate diffuse ridges.

Other mass movement formations are debris-avalanches (DA; Figure 4 (a)) punctually located on the lateral moraines in both valleys. Usually these formations are small in size, however we identified a major avalanche in the left lateral moraine of the Gredos gorge, close to the Cervunal area. These landforms exhibit semi-circular scarps on the headwalls of mass-wasting deposits reaching the floor of the valley. The typical fan-like planform of the deposit has been hidden by modern fluvial activity. The morphology of the deposits consists of a system of stepped lobes indicates that the avalanche has been reactivated several times in the past.

Finally, in areas of weathered rocks (grus) and concentrations of fine-grain materials (i.e. subglacial till and hydromorphic soils), solifluction-gelifluction phenomena are frequent and lobes, sheets, and tongues of small dimensions (2–5 m) are formed.

### 4.4. Structural landforms

In the upper sector of both gorges, we recognized a wide variety of structural landforms, such as fracture zones or corridors and fault-line escarpments or thresholds (Figures 2, 6(a) and 6(d)). These features are determined by the local lithology and tectonic layout of the regional and local faults. Fracture zones and structural corridors are linear negative-relief features that connect the summit area with the cirque floor with no preferential orientation. The most impressive structural corridors can reach ~500 m in length, ~80 m in width and ~10 m in depth. The majority are covered by unconsolidated debris of different grain size on their floors and occasionally they can contain glacial till and periglacial protalus or pronival ramparts. Some of these landforms have been identified as frequent snow avalanche paths in the area (Soteres, Pedraza, et al., 2020).

### 4.5. Glaciofluvial and fluvial landforms

Glaciofluvial landforms are residual outwash plains (proglacial alluvial plains and proglacial alluvial fans, PAf) dissected by postglacial river channels. These

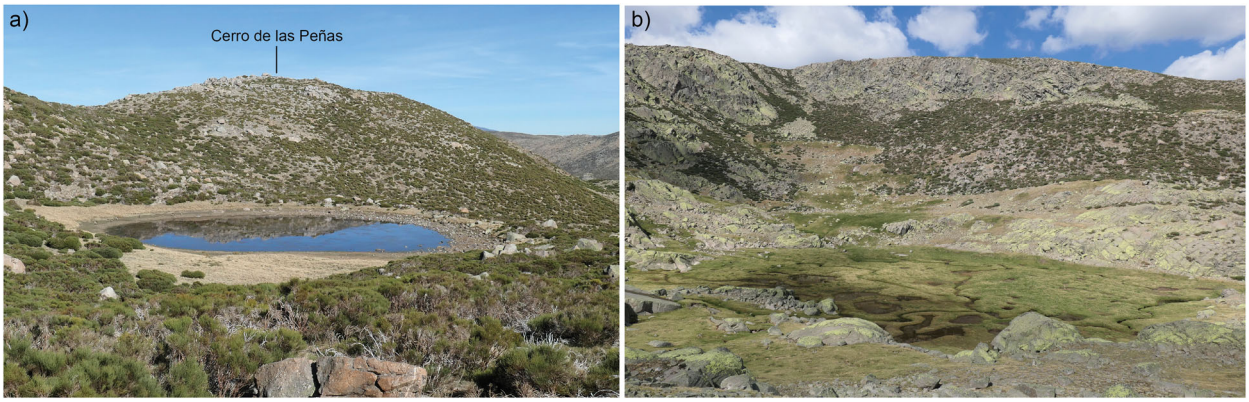


**Figure 7.** (a) Seasonal proglacial moraine-dammed pond type of the Laguna del Cervunal, view from the SW (see Figure 4). (b) Peaty system on the former seasonal cirque pond in Las Lagunillas site, view from the SE (see Figure 3).

postglacial fluvial processes show total continuity with the previous glaciofluvial processes and are represented by the current river channel and adjacent alluvial plain and, locally, alluvial fans (Af).

The main streams flow from headwall lakes following the valley floor until they cut through the relict frontal moraines in both gorges. Upstream, the main river is predominantly linear, channeled in the ice-sculpted topography. Downstream, the river channel planform describes diffuse meanders over minor alluvial terraces (T), forming fluvial bars locally (Figures 4 (b) and 4 (c)). All these fluvial and glaciofluvial morphologies are embedded in the bottom of the former glacial valley on bedrock polished surfaces (PS) or previous surficial deposits.

### 4.6. Lacustrine landforms

Lacustrine features are mainly composed of lakes and peaty system. The lakes are small to very small (ponds), perennial or seasonal covering 8 ha in Laguna Grande (Gredos Cirque) to 0.3 ha in Laguna Mediana (Pinar Cirque), and their depth range from 0.5 m in Las Lagunillas to 9.5 m in Laguna Cimera (both in the Pinar Cirque) (Figures 3 and 7(a) and 7(b)).

The interfluve between the valleys hosts the only proglacial moraine-dammed pond in the area, the Laguna del Cervunal (Figure 7a). Most of the bedrock-dammed lakes and ponds (12 in total) are in the cirques that form the headwalls of both gorges, where over-deepened rocky basins were excavated by glacial processes (cirque lakes type).

Peaty system is created by the sediment overfilling of former lacustrine basins or similar depressions. The resulting landform is defined by a flat surface colonized by herbaceous vegetation. Mostly without well-developed soils and with small grasslands of *Nardus stricta* and psicroxerophytic meadows (locally termed *cervunales* and *navas*). Major peaty systems are often associated with the proximal slopes of moraine limits where they most likely formed proglacial lakes in the past.

The most extensive peaty system or *navas* in the area are the Prados del Cervunal meadows, dammed for the moraines of Pinar and Gredos paleoglaciers (Figure 4a). This peaty system is like Navamuño, other lateral complexes located 40 km west in Cuerpo de Hombre Valley (Carrasco et al., 2018; Turu et al., 2018).

## 5. Conclusions

Detailed geomorphological mapping of two of the major gorges of the High Gredos Massif, called the Gredos and Pinar valleys, was performed using aerial orthophotographs and LiDAR-derived DTMs. The study area is dominated by a wide variety of glacial landforms, especially ice-marginal features, such as moraine ridges, ice-sculped topography and aligned boulder trains. Other landforms associated with periglacial processes, such as protalus ramparts, are represented in the headwalls of both gorges. In combination, glacial and periglacial landforms offer insight into the structure of local glacial activity since the last glaciation.

Major glacial limits clearly delimitate former glacier geometry during the local LGM and possibly during the Late Glacial and Holocene periods as well. According to our interpretation, both Gredos and Pinar paleoglaciers may have experienced a rapid retreat during the last deglaciation following a similar sequence of glacial events to other paleoglaciers in the region.

Our main map provides a new spatial frame where chronological analyses of the glacial landforms can be performed, contributing to the assessment of potential mechanisms operating behind past climate changes at a regional and hemispheric scale.

## Software

The spatial information analysis was carried out on ArcGIS 10.4 software (academic licenses from Universidad Complutense de Madrid, UCM). Hillshade extraction from the digital elevation model was

performed with Surfer 15. Final maps were produced with Adobe Illustrator CC 2019.

## Acknowledgements

Authors acknowledge the help and assistance received from the Sierra de Gredos Regional Park, the Environmental Department of the Junta de Castilla y León (JCyL) and the Gabinete Lingüístico of the Universidad Complutense de Madrid (UCM). Additionally, we would like to thank the Editor Dr Paul Dunlop and the reviewers Drs José M Fernández-Fernández, David Palacios and Giedre Beconyte for their remarkable contributions for improving the manuscript and map.

## Disclosure statement

No potential conflict of interest was reported by the authors.

## Funding

This work was supported by the Spanish Ministry of Science and Innovation (Spanish initials: MINECO; project CGL2016-78380-P), University of Castilla–La Mancha Research Group (UCLM, project 2020-GRIN-28992) and the Chilean Ph.D. Fellowship CONICYT #21161417 and the ANID Millennium Science Initiative/Millennium Nucleus Paleoclimate.

## ORCID

*Rosa M. Carrasco* http://orcid.org/0000-0001-8762-6951
*Rodrigo L. Soteres* http://orcid.org/0000-0003-3647-5342
*Javier Pedraza* http://orcid.org/0000-0002-3445-8111
*Javier Fernández-Lozano* http://orcid.org/0000-0001-9741-3917
*Valentí Turu* http://orcid.org/0000-0002-5087-2064
*José Antonio López-Sáez* http://orcid.org/0000-0002-3122-2744
*Theodoros Karampaglidis* http://orcid.org/0000-0001-5626-4548
*José Luis Granja-Bruña* http://orcid.org/0000-0001-8741-5388
*Alfoso Muñoz-Martín* http://orcid.org/0000-0002-5302-5119

## References

Acaso, E., Ruíz-Zapata, M. B., Pedraza-Gilsanz, J., & de Dios Centeno-Carrillo, J. (1986). Contribución al estudio del periglaciarismo en la Sierra de Gredos. *Cadernos do Laboratorio Xeolóxico de Laxe*, *10*, 115–132. https://ruc.udc.es/dspace/bitstream/handle/2183/5953/CA-10-7.pdf?sequence=1&isAllowed=y

AEMET/IPMA. (2011). *Atlas Climático Ibérico/iberian Climate Atlas*. Agencia Estatal de Meteorología (AEMET) and Instituto Português do Mar e da Atmosfera (IPMA). http://www.aemet.es/es/conocermas/recursos_en_linea/publicaciones_y_estudios/publicaciones/detalles/Atlas-climatologico

Balco, G. (2011). Contributions and unrealized potential contributions of cosmogenic-nuclide exposure dating to glacier chronology, 1990–2010. *Quaternary Science Reviews*, *30*(1–2), 3–27. https://doi.org/10.1016/j.quascirev.2010.11.003

Ballantyne, C. K., & Benn, D. I. (1994). Glaciological constraints on protalus rampart development. *Permafrost and Periglacial Processes*, *5*(3), 145–153. https://doi.org/10.1002/ppp.3430050304

Baysselance, E. (1884). Quelques traces glaciaires en Espagne. *Annuaire du Club Alpin Française*, *10*, 410–416.

Bendle, J. M., Thorndycraft, V. R., & Palmer, A. P. (2017). The glacial geomorphology of the lago Buenos Aires and lago pueyrredón ice lobes of central patagonia. *Journal of Maps*, *13*(2), 654–673. https://doi.org/10.1080/17445647.2017.1351908

Campos, N., Tanarro, L. M., & Palacios, D. (2018). Geomorphology of glaciated gorges in a granitic massif (Gredos range, central Spain). *Journal of Maps*, *14*(2), 321–329. https://doi.org/10.1080/17445647.2018.1468829

Carrasco, R. M., Pedraza, J., Domínguez-Villar, D., Villa, J., & Willenbring, J. K. (2013). The plateau glacier in the Sierra de Bejar (Iberian Central System) during its maximum extent. Reconstruction and chronology. *Geomorphology*, *196*, 83–93. https://doi.org/10.1016/j.geomorph.2012.03.019

Carrasco, R. M., Pedraza, J., Domínguez-Villar, D., Willenbring, J. K., & Villa, J. (2013). Supraglacial debris supply in the Cuerpo de Hombre paleoglacier (Spanish Central System): Reconstruction and interpretation of a rock avalanche event. *Geografiska Annaler: Series A, Physical Geography*, *95*(3), 211–226. https://doi.org/10.1111/geoa.12010

Carrasco, R. M., Pedraza, J., Domínguez-Villar, D., Willenbring, J. K., & Villa, J. (2015). Sequence and chronology of the Cuerpo de Hombre paleoglacier (Iberian Central System) during the last glacial cycle. *Quaternary Science Reviews*, *129*, 163–177. https://doi.org/10.1016/j.quascirev.2015.09.021

Carrasco, R. M., Turu, V., Pedraza, J., Muñoz-Martín, A., Ros, X., Sánchez, J., Ruiz-Zapata, B., Olaiz, A. J., & Herrero-Simón, R. (2018). Near surface geophysical analysis of the Navamuño depression (Sierra de Béjar, Iberian Central System): Geometry, sedimentary infill and genetic implications of tectonic and glacial footprint. *Geomorphology*, *315*, 1–16. https://doi.org/10.1016/j.geomorph.2018.05.003

Chandler, B., Lovell, H., Boston, C. M., Lukas, S., Barr, I. D., Benediktsson, Í. Ö., Benn, D. I., Clark, C. D., Darvill, C. M., Evans, D. J. A., Ewertowski, M. W., Loibl, D., Margold, M., Otto, J.-C., Roberts, D. H., Stokes, C. R., Storrar, R. D., & Stroeven, A. P. (2018). Glacial geomorphological mapping: A review of approaches and frameworks for best practice. *Earth-Science Reviews*, *185*, 806–846. https://doi.org/10.1016/j.earscirev.2018.07.015

CHD. (2012). Propuesta de Proyecto de Plan Hidrológico. Anejos. 3. Zonas Protegidas, Código 3, Cabecera del río Tormes. Ministerio de Agricultura Alimentación y Medio Ambiente, Gobierno de España, Madrid. https://www.chduero.es/anejo3

Darvill, C. M., Stokes, C. R., Bentley, M. J., & Lovell, H. (2014). A glacial geomorphological map of the southernmost ice lobes of Patagonia: The Bahía Inútil – San Sebastián, Magellan, Otway, Skyring and Río Gallegos lobes. *Journal of Maps*, *10*(3), 500–520. https://doi.org/10.1080/17445647.2014.890134

de Prado, C. (1862). Reseña geológica de la provincia de Ávila y de la parte occidental de la de León. Comisión Nacional del Mapa Geológico de España, Junta General

Estadística, Madrid. http://bdh-rd.bne.es/viewer.vm?id=0000052546&page=1

De Vicente, G., Cloetingh, S., Van Wees, J. D., & Cunha, P. P. (2011). Tectonic classification of Cenozoic Iberian foreland basins. *Tectonophysics*, *502*(1–2), 38–61. https://doi.org/10.1016/j.tecto.2011.02.007

Demek, J. (Ed.). (1972). Manual of detailed geomorphological mapping. IGU Commission for Geomorphological Mapping, Academia, Prague.

Durán, L., Sánchez, E., & Yagüe, C. (2013). Climatology of precipitation over the Iberian Central System mountain range. *International Journal of Climatology*, *33*(9), 2260–2273. https://doi.org/10.1002/joc.3602

Evans, I. S. (2012). Geomorphometry and landform mapping: What is a landform? *Geomorphology*, *137*(1), 94–106. https://doi.org/10.1016/j.geomorph.2010.09.029

Evans, I. S., & Cox, N. J. (1974). Geomorphometry and the operational definition of cirques. *Area*, *6*, 150–153. https://www.jstor.org/stable/20000855

Federal Geographic Data Committee (FGDC). (2006). FGDC digital cartographic standard for geologic map symbolization: Reston, VA, Federal Geographic Data Committee Document Number FGDC-STD-013-2006, 290 p., 2 plates. https://ngmdb.usgs.gov/fgdc_gds/geolsymstd/fgdc-geolsym-all.pdf

Fernández-Lozano, J., Carrasco, R. M., Pedraza, J., & Bernardo-Sánchez, A. (2020). The anthropic landscape imprint around one of the largest Roman hydraulic gold mines in Europe: Sierra del Teleno (NW Spain). *Geomorphology*, *357*, 107094. https://doi.org/10.1016/j.geomorph.2020.107094

Fernández-Lozano, J., Gutiérrez-Alonso, G., & Fernández-Morán, M. Á. (2015). Using airborne LiDAR sensing technology and aerial orthoimages to unravel roman water supply systems and gold works in NW Spain (Eria valley, León). *Journal of Archaeological Science*, *53*, 356–373. https://doi.org/10.1016/j.jas.2014.11.003

GEODE. (2004). *Cartografía geológica digital continua a escala 1:50.000*. Instituto Geológico y Minero de España (IGME). http://info.igme.es/cartografiadigital/geologica/Geode.aspx

Gosse, J. C., & Phillips, F. M. (2001). Terrestrial in situ cosmogenic nuclides: Theory and application. *Quaternary Science Reviews*, *20*(14), 1475–1560. https://doi.org/10.1016/S0277-3791(00)00171-2

Hesse, R. (2010). LiDAR-derived local relief models – A new tool for archaeological prospection. *Archaeological Prospections*, *17*, 67–72. https://doi.org/10.1002/arp.374

Huget del Villar, E. (1915). Los glaciares de Gredos. *Boletin de La Real Sociedad Española de Historia Natural*, *15*, 379–390.

Hughes, P., & Woodward, J. (2008). Timing of glaciation in the Mediterranean mountains during the last cold stage. *Journal of Quaternary Science*, *23*(6–7), 575–588. https://doi.org/10.1002/jqs.1212

Hurrell, J. W. (1995). Decadal trends in the North Atlantic oscillation: Regional temperatures and precipitation. *Science*, *269*(5224), 676–679. https://doi.org/10.1126/science.269.5224.676

Hurrell, J. W., & Deser, C. (2009). North Atlantic climate variability: The role of the North Atlantic oscillation. *Journal of Marine Systems*, *78*(1), 28–41. https://doi.org/10.1016/j.jmarsys.2008.11.026

IGN-CNIG. *Centro Nacional de Información Geográfica*. http://centrodedescargas.cnig.es/CentroDescargas/inicio.do

IGN-IBERPIX. *Visor geográfico español*. http://www.ign.es/iberpix2/visor/#

Ivy-Ochs, S., & Kober, F. (2008). Surface exposure dating with cosmogenic nuclides. *E&G Quaternary Science Journal*, *57*(1/2), 179–209. https://doi.org/10.3285/eg.57.1-2.7

Kokalj, Z., Zakšek, K., & Oštir, K. (2011). Application of sky-view factor for the visualisation of historic landscape features in lidar-derived relief models. *Antiquity*, *85*(327), 263–273. https://doi.org/10.1017/S0003598X00067594

Leger, T. P. M., Hein, A. S., Bingham, R. G., Martini, M. A., Soteres, R. L., Sagredo, E. A., & Martínez, O. A. (2020). The glacial geomorphology of the Río Corcovado, Río Huemul and Lago Palena/General Vintter valleys, northeastern Patagonia (43°S, 71°W). *Journal of Maps*, *16*(2), 651–668. https://doi.org/10.1080/17445647.2020.1794990

Lindholm, M. S., & Heyman, J. (2016). Glacial geomorphology of the Maidika region, Tibetan Plateau. *Journal of Maps*, *12*(5), 797–803. https://doi.org/10.1080/17445647.2015.1078182

López-Moreno, J. I., Vicente-Serrano, S. M., Morán-Tejeda, E., Lorenzo-Lacruz, J., Kenawy, A., & Beniston, M. (2011). Effects of the North Atlantic Oscillation (NAO) on combined temperature and precipitation winter modes in the Mediterranean mountains: Observed relationships and projections for the 21st century. *Global and Planetary Change*, *77*(1–2), 62–76. https://doi.org/10.1016/j.gloplacha.2011.03.003

López-Sáez, J. A., Carrasco, R. M., Turu, V., Ruiz-Zapata, B., Gil-García, M. J., Luelmo-Lautenschlaeger, R., Pérez-Díaz, S., Alba-Sánchez, F., Abel-Schaad, D., Ros, X., & Pedraza, J. (2020). Late Glacial-early holocene vegetation and environmental changes in the western Iberian Central System inferred from a key site: The Navamuño record, Béjar range (Spain). *Quaternary Science Reviews*, *230*, 106167. https://doi.org/10.1016/j.quascirev.2020.106167

Mackintosh, A. N., Anderson, B. M., & Pierrehumbert, R. T. (2017). Reconstructing climate from glaciers. *Annual Review of Earth and Planetary Sciences*, *45*(1), 649–680. https://doi.org/10.1146/annurev-earth-063016-020643

Marshall, J., Johnson, H., & Goodman, J. (2001). A study of the interaction of the North Atlantic oscillation with ocean circulation. *Journal of Climate*, *14*(7), 1399–1421. https://doi.org/10.1175/1520-0442(2001)014<1399:ASOTIO>2.0.CO;2

Martínez de Pisón, E., & Muñoz-Jiménez, J. (1972). Observaciones sobre la morfologia del Alto Gredos. *Estudios Geográficos*, *33*(129), 597–690.

Martínez de Pisón, E., & Palacios, D. (1997). Significado del episodio glaciar en la evolución morfológica y en el paisaje de la Sierra de Gredos, Sistema Central. In A. Gómez Ortiz, & A. Pérez Albertí (Eds.), *Las huellas glaciares de las montañas españolas* (pp. 163–207). Santiago de Compostela.

Matthews, J. A., Wilson, P., & Mourne, R. W. (2017). Landform transitions from pronival ramparts to moraines and rock glaciers: A case study from the Smørbotn cirque, Romsdalsalpane, southern Norway. *Geografiska Annaler: Series A, Physical Geography*, *99*(1), 15–37. https://doi.org/10.1080/04353676.2016.1256582

Muñoz, J., Palacios, D., & Marcos, J. (1995). The influence of the geomorphologic heritage on present slope dynam. The Gredos Cirque, Spain. *Pirineos*, *145–146*(0), 35–63. http://pirineos.revistas.csic.es/index.php/pirineos/article/view/146/145

Muñoz-Salinas, E., Castillo, M., Sanderson, D., & Kinnaird, T. (2013). Unraveling paraglacial activity on Sierra de

Gredos, Central Spain: A study based on geomorphic markers, stratigraphy and OSL. *Catena*, *110*, 207–214. https://doi.org/10.1016/j.catena.2013.06.018

Ninyerola, M., Pons, X., & Roure, J. M. (2005). Atlas Climático Digital de la Península Ibérica. Metodología y aplicaciones en bioclimatología y geobotánica. Universidad Autónoma de Barcelona, Bellaterra. http://opengis.uab.es/wms/iberia/espanol/es_referencies.htm

Obermaier, H., & Carandell, J. (1915). Datos para la climatologia cuaternaria de España. *Boletin de La Real Sociedad Española de Historia Natural*, *15*, 402–411.

Obermaier, H., & Carandell, J. (1916). Contribucion al estudio del glaciarismo cuaternario de la Sierra de Gredos. *Trabajos Del Museo Nacional de Ciencias Naturales*, *14*, 54.

Oerlemans, J. (2005). Extracting a climate signal from 169 glacier records. *Science*, *308*(5722), 675–677. https://doi.org/10.1126/science.1107046

Oliva, M., Palacios, D., Fernández-Fernández, J. M., Rodríguez-Rodríguez, L., García-Ruiz, J. M., Andrés, N., Carrasco, R. M., Pedraza, J., Pérez-Alberti, A., Valcárcel, M., & Hughes, P. D. (2019). Late quaternary glacial phases in the Iberian Peninsula. *Earth-Science Reviews*, *192*(March), 564–600. https://doi.org/10.1016/j.earscirev.2019.03.015

Oliva, M., Serrano, E., Gómez-Ortiz, A., González-Amuchastegui, M. J., Nieuwendam, A., Palacios, D., Pérez-Alberti, A., Pellitero-Ondicol, R., Ruiz-Fernández, J., Valcárcel, M., Vieira, G., & Antoniades, D. (2016). Spatial and temporal variability of periglaciation of the Iberian Peninsula. *Quaternary Science Reviews*, *137*, 176–199. https://doi.org/10.1016/j.quascirev.2016.02.017

Palacios, D., Andrés, N., Marcos, J., & Vázquez-Selem, L. (2012). Maximum glacial advance and deglaciation of the Pinar Valley (Sierra de Gredos, Central Spain) and its significance in the Mediterranean context. *Geomorphology*, *177–178*, 51–61. https://doi.org/10.1016/j.geomorph.2012.07.013

Palacios, D., de Marcos, J., & Vázquez-Selem, L. (2011). Last glacial maximum and deglaciation of Sierra de Gredos, central Iberian Peninsula. *Quaternary International*, *233* (1), 16–26. https://doi.org/10.1016/j.quaint.2010.04.029

Palacios, D., & Marcos, J. (1996). La elaboración de la cartografía de riesgos geomorfológicos y su aplicación en áreas de alta montaña. *Serie Geográfica*, *6*, 59–97. https://dialnet.unirioja.es/servlet/articulo?codigo=1907800&orden=388860&info=link

Pearce, D. M., Ely, J. C., Barr, I. D., & Boston, C. M. (2017). Section 3.4.9: Glacier Reconstruction. In: Cook, S. J., Clarke, L. E., & Nield, J. M. (Eds.), *Geomorphological techniques* (Online Edition) (pp. 1–16). British Society for Geomorphology. https://www.geomorphology.org.uk/geomorph_techniques

Pedraza, J. (1994). El Sistema Central Español. In M. Gutiérrez-Elorza (Ed.), *Geomorfología de España* (pp. 63–100). Editorial Rueda.

Pedraza, J., Carrasco, R. M., Domínguez-Villar, D., & Villa, J. (2013). Late Pleistocene glacial evolutionary stages in the Gredos Mountains (Iberian Central System). *Quaternary International*, *302*, 88–100. https://doi.org/10.1016/j.quaint.2012.10.038

Pedraza, J., Carrasco, R. M., Villa, J., Soteres, R. L., Karampaglidis, T., & Fernández-Lozano, J. (2019). Cirques in the Sierra de Guadarrama and7 Somosierra mountains (Iberian Central System): Shape, size and controlling factors. *Geomorphology*, *341*, 153–168. https://doi.org/10.1016/j.geomorph.2019.05.024

Pedraza, J., & Fernández, P. (1981). Cuaternario del Mapa Geológico de de Bohovo. En P. Ruiz y V. Gabaldón (supervis.), *Mapa Geológico de Bohoyo*. Serie MAGNA, H-577, IGME. http://info.igme.es/cartografiadigital/geologica/Geo50.aspx?language=en

Penck, A. (1894). Studien uber das Klima Spanien whärend der jüngeren Tertiärperiode und der Diluvialperiode. *Zeitschrift der Gesellschaft für Erdkunde zur Berlin*, *29*, 109–141. https://www.digizeitschriften.de/dms/img/?PID=PPN391365657_1894_0029%7CLOG_0017

Roe, G. H., Baker, M. B., & Herla, F. (2017). Centennial glacier retreat as categorical evidence of regional climate change. *Nature Geoscience*, *10*(2), 95–99. https://doi.org/10.1038/ngeo2863

Sánchez-López, G., Hernández, A., Pla-Rabes, S., Toro, M., Granados, I., Sigró, J., & Giralt, S. (2015). The effects of the NAO on the ice phenology of Spanish alpine lakes. *Climatic Change*, *130*(2), 101–113. https://doi.org/10.1007/s10584-015-1353-y

Sánchez-López, G., Hernández, A., Pla-Rabes, S., Trigo, R. M., Toro, M., Granados, I., & Giralt, S. (2016). Climate reconstruction for the last two millennia in central Iberia: The role of East Atlantic (EA), North Atlantic Oscillation (NAO) and their interplay over the Iberian Peninsula. *Quaternary Science Reviews*, *149*, 135–150. https://doi.org/10.1016/j.quascirev.2016.07.021

Sancho, L. G., Palacios, D., de Marcos, J., & Valladares, F. (2001). Geomorphological significance of lichen colonization in a present snow hollow: Hoya del Cuchillar de las Navajas, Sierra de Gredos (Spain). *CATENA*, *43*(4), 323–340. https://doi.org/10.1016/S0341-8162(00)00131-4

Schmieder, O. (1915). Die Sierra de Gredos. *Mitteilungen der Geographischen Gesellschaft in München*, Zehnter Band, *10* (1), 60 pp.

Seijmonsbergen, A. C. (2013). The modern geomorphological map. In: Shroder, J. (EditorinChief), Switzer, A. D., & Kennedy, D. M. (Eds.), *Treatise on Geomorphology*. Academic Press, vol.14, Methods in Geomorphology, pp. 35–52. https://doi.org/10.1016/B978-0-12-374739-6.00371-7

Shakesby, R. A. (1997). Pronival (protalus) ramparts: A review of forms, processes, diagnostic criteria and p alaeoenvi ronmental implications. *Progress in Physical Geography: Earth and Environment*, *21*(3), 394–418. https://doi.org/10.1177/030913339702100304

Smith, M. J., Rose, J., & Booth, S. (2006). Geomorphological mapping of glacial landforms from remotely sensed data: An evaluation of the principal data sources and an assessment of their quality. *Geomorphology*, *76*(1-2), 148–165. https://doi.org/10.1016/j.geomorph.2005.11.001

Soteres, R. L., Pedraza, J., & Carrasco, R. M. (2020). Snow avalanche susceptibility of the Circo de Gredos (Iberian Central System, Spain). *Journal of Maps*, *16*(2), 155–165. https://doi.org/10.1080/17445647.2020.1717655

Soteres, R. L., Peltier, C., Kaplan, M. R., & Sagredo, E. A. (2020). Glacial geomorphology of the Strait of Magellan ice lobe, southernmost Patagonia, South America. *Journal of Maps*, *16*(2), 299–312. https://doi.org/10.1080/17445647.2020.1736197

Sutherland, D. G. (1984). Modern glacier characteristics as a basis for inferring former climates with particular reference to the Loch Lomond Stadial. *Quaternary Science Reviews*, *3*(4), 291–309. https://doi.org/10.1016/0277-3791(84)90010-6

Turu, V., Carrasco, R. M., Pedraza, J., Ros, X., Ruiz-Zapata, B., Soriano-López, J. M., Mur-Cacuho, E., Pélachs-Mañosa, A., Muñoz-Martín, A., Sánchez, J., & Echeverria-Moreno, A. (2018). Late glacial and post-glacial deposits of the Navamuño peatbog (Iberian Central

System): Chronology and paleoenvironmental implications. *Quaternary International*, *470*, 82–95. https://doi.org/10.1016/j.quaint.2017.08.018

Verstappen, H. T. (2011). Old and new trends in geomorphological and landform mapping. *Developments in Earth Surface Processes*, *15*(1952), 13–38. https://doi.org/10.1016/B978-0-444-53446-0.00002-1

Vicente-Serrano, S. M., Beguería, S., López-Moreno, J. I., El Kenawy, A. M., & Angulo-Martı, M. (2009). Daily atmospheric circulation events and extreme precipitation risk in northeast Spain: Role of the North Atlantic Oscillation, the Western Mediterranean Oscillation, and the Mediterranean Oscillation. *Journal of Geophysical Research*, *114*(D8), 1–19. https://doi.org/10.1029/2008JD011492

Vidal Box, C. (1932). Morfología glacial cuaternaria del macizo Oriental de la Sierra de Gredos. *Boletín de La Real Sociedad Española de Historia Natural*, *32*, 117–135.

Vidal Box, C. (1936). Contribución al conocimiento morfológico del segmento occidental de la Sierra de Gredos (Bohoyo). *Boletin de La Real Sociedad Española de Historia Natural*, *36*, 17–31.

Winkler, S. (2018). Investigating Holocene mountain glaciations: A plea for the supremacy of glacial geomorphology when reconstructing glacier chronologies. *Erdkunde*, *72* (3). https://doi.org/10.3112/erdkunde.2018.03.04

Zasadni, J., & Kłapyta, P. (2014). The Tatra mountains during the last glacial maximum. *Journal of Maps*, *10* (3), 440–456. doi:10.1080/17445647.2014.885854